



Published in final edited form as:

*Kidney Int.* 2014 July ; 86(1): 118–126. doi:10.1038/ki.2014.5.

## The cooperative roles of the dopamine receptors, D<sub>1</sub>R and D<sub>5</sub>R, on the regulation of renal sodium transport

John J. Gildea, PhD<sup>1</sup>, Ishan T. Shah, BS<sup>1</sup>, Robert Van Sciver, BS<sup>1</sup>, Jonathan A. Israel, MD<sup>1</sup>, Christoph Enzensperger, PhD<sup>2</sup>, Helen E. McGrath, BA<sup>1</sup>, Pedro A. Jose, MD, PhD<sup>3</sup>, and Robin A. Felder, PhD<sup>1</sup>

<sup>1</sup>The University of Virginia Health System, Department of Pathology, Charlottesville, VA

<sup>2</sup>Institut für Pharmazie, Lehrstuhl für Pharmazeutische/Medizinische Chemie, FriedrichSchiller-Universität Jena, Jena, Germany

<sup>3</sup>University of Maryland School of Medicine, Departments of Medicine and Physiology, Baltimore, MD

### Abstract

Determining the individual roles of the two dopamine D<sub>1</sub>-like receptors (D<sub>1</sub>R and D<sub>5</sub>R) on sodium transport in the human renal proximal tubule has been complicated by their structural and functional similarity. Here we used a novel D<sub>5</sub>R-selective antagonist (LE-PM436) and D<sub>1</sub>R or D<sub>5</sub>R-specific gene silencing to determine second messenger coupling pathways and heterologous receptor interaction between the two receptors. D<sub>1</sub>R and D<sub>5</sub>R co-localized in renal proximal tubule cells and physically interact, as determined by co-immunoprecipitation and FRET microscopy. Stimulation of renal proximal tubule cells with fenoldopam (D<sub>1</sub>R/D<sub>5</sub>R agonist) led to both adenylyl cyclase and phospholipase C (PLC) activation using real-time FRET biosensors ICUE3 and CYPHR, respectively. Fenoldopam increased cAMP accumulation and PLC activity and inhibited both NHE3 and NaKATPase activities. LE-PM436 and D<sub>5</sub>R siRNA blocked the fenoldopam-stimulated PLC pathway but not cAMP accumulation, while D<sub>1</sub>R siRNA blocked both fenoldopam-stimulated cAMP accumulation and PLC signaling. Either D<sub>1</sub>R or D<sub>5</sub>R siRNA, or LE-PM436 blocked the fenoldopam dependent inhibition of sodium transport. Further studies using the cAMP-selective D<sub>1</sub>R/D<sub>5</sub>R agonist SKF83822 and PLC-selective D<sub>1</sub>R/D<sub>5</sub>R agonist SKF83959 confirmed the cooperative influence of the two pathways on sodium transport. Thus, D<sub>1</sub>R and D<sub>5</sub>R interact in the inhibition of NHE3 and NaKATPase activity, the D<sub>1</sub>R primarily by cAMP, while the D<sub>1</sub>R/D<sub>5</sub>R heteromer modulates the D<sub>1</sub>R effect through a PLC pathway.

---

Users may view, print, copy, and download text and data-mine the content in such documents, for the purposes of academic research, subject always to the full Conditions of use:[http://www.nature.com/authors/editorial\\_policies/license.html#terms](http://www.nature.com/authors/editorial_policies/license.html#terms)

Correspondence to be sent to: Robin A. Felder, Ph.D. The University of Virginia, P.O. Box 801400, Charlottesville, VA 22908, rfelder@virginia.edu, Ph 434-466-1131, Fax 434-924-5718.

Supplementary information is available at *Kidney International* website.

**Disclosure:** The authors have no COI to disclose.

## Introduction

Dopamine produced in the renal proximal tubule from circulating L-DOPA acts as a paracrine and autocrine hormone to regulate greater than 50% of sodium excretion in animals and humans on moderately high salt intake.<sup>1-3</sup> Dopamine exerts its natriuretic effect by acting with cell surface receptors and intracellular pathways to stimulate intracellular adenylyl cyclase (AC) and phospholipase C (PLC) activities and inhibit sodium transport. There are 5 dopamine receptors expressed in renal proximal tubule cells (RPTCs): the D<sub>1</sub>-like (D<sub>1</sub>R and D<sub>5</sub>R) and the D<sub>2</sub>-like (D<sub>2</sub>R, D<sub>3</sub>R, D<sub>4</sub>R) receptors, that interact with other systems including the renin angiotensin system to regulate renal sodium excretion.<sup>4, 5</sup> In mice, a deficiency in local production of dopamine results in hypertension and a decrease in longevity.<sup>6</sup>

The D<sub>5</sub>R is of particular interest because it has a 10-fold higher affinity for dopamine than D<sub>1</sub>R but has an 80% homology in the transmembrane domain and a 30% homology in the N and C termini.<sup>7</sup> Both D<sub>1</sub>R and D<sub>5</sub>R are linked to G<sub>αs</sub>.<sup>7</sup> The D<sub>1</sub>R, but not D<sub>5</sub>R, also couples to G<sub>O</sub><sup>8</sup> and G<sub>Olf</sub><sup>9</sup> while the D<sub>5</sub>R but not D<sub>1</sub>R, couples to G<sub>Z</sub><sup>10</sup> and G<sub>α12/13</sub>.<sup>11</sup> In the rat forebrain, D<sub>1</sub>-like receptors couple to both G<sub>αs</sub> and G<sub>αq</sub> while in the rat hippocampus and amygdala, D<sub>1</sub>-like receptors couple only to G<sub>αq</sub>.<sup>12</sup> In contrast, in hippocampal and brain cortical and striatal tissues of D<sub>5</sub>R<sup>-/-</sup> mice, PLC is not activated in the brain following stimulation with dopamine, the non-selective D<sub>1</sub>R/D<sub>5</sub>R agonist SKF38393, or the PLC-selective D<sub>1</sub>R/D<sub>5</sub>R agonist SKF83959.<sup>13, 14</sup> This suggests that in specific areas in the brain, D<sub>1</sub>R couples preferentially to AC and the D<sub>5</sub>R couples to PLC.<sup>15</sup>

Which D<sub>1</sub>-like receptor subtype is linked to G<sub>αq</sub> and PLC in cells in which both D<sub>1</sub>-like receptors are expressed is not clear. While the D<sub>1</sub>R and D<sub>5</sub>R may have different anatomical distributions in the brain,<sup>16</sup> both the renal D<sub>1</sub>R and D<sub>5</sub>R are found in specific nephron segments (proximal convoluted and straight tubules, thick ascending limb of Henle, distal convoluted tubule and cortical collecting duct), suggesting a possible interaction between these receptors.<sup>17</sup> We have reported that in renal cortical membranes, D<sub>1</sub>-like receptors are linked to G<sub>αq</sub> and that PLC activity can be stimulated by D<sub>1</sub>-like receptors independent of AC.<sup>18</sup> Others have reported that the linkage of renal D<sub>1</sub>-like receptors to PLC may be observed to a greater extent in rats fed a high salt diet.<sup>19</sup> We have previously shown that both D<sub>1</sub>R and D<sub>5</sub>R are expressed in RPTCs.<sup>20</sup> However, little is known about their physical association and the relative contribution of each receptor on AC and PLC signaling in a single cell type. Studying the D<sub>1</sub>R and D<sub>5</sub>R in a single cell type is important because similarities and differences in signaling pathways may be tissue specific (vide supra).

Deletion of either D<sub>1</sub>R (D<sub>1</sub>R<sup>-/-</sup>)<sup>21</sup> or D<sub>5</sub>R (D<sub>5</sub>R<sup>-/-</sup>)<sup>22</sup> gene in mice results in elevation of blood pressure. Increased salt intake further increases the high blood pressure of D<sub>5</sub>R<sup>-/-</sup> mice.<sup>23, 24</sup> The effect of salt intake on blood pressure in D<sub>1</sub>R<sup>-/-</sup> mice has not been reported. Since both the D<sub>1</sub>R and D<sub>5</sub>R are important in the control of blood pressure,<sup>3-5, 17, 24-26</sup> in part by regulation of renal sodium transport, we further examined the AC and PLC pathways and their relationship to NHE3 and NaKATPase using agonists that have selectivity to D<sub>5</sub>R, AC, and PLC and silencing of D<sub>1</sub>R or D<sub>5</sub>R (see our model display of these pathways and agonists). These studies were performed using human RPTCs with

normal D<sub>1</sub>R and AC coupling, since a fully functional D<sub>1</sub>R is necessary for D<sub>1</sub>R/D<sub>5</sub>R agonist-mediated inhibition of NHE3 and NaKATPase.<sup>27</sup>

## Results

We demonstrated that the D<sub>1</sub>R and D<sub>5</sub>R were physically associated in the same macromolecular protein complex using a co-immunoprecipitation method (Figure 1). We further demonstrated that the amount of D<sub>5</sub>R protein pulled down using the D<sub>1</sub>R antibody was increased following fenoldopam (FEN, 1 μmol/L, 30-min) stimulation (P<0.001, N=6, one immunoblot is shown in Figure 1 inset). Further evidence of association is seen by reciprocal co-immunoprecipitation with D<sub>1</sub>R and D<sub>5</sub>R, and adequate washing is demonstrated by inclusion of the appropriate non-specific IgG antibody controls in the initial immunoprecipitation (Figure S1).

Confocal microscopy was used to determine if the two receptors co-localize in renal cortical proximal tubules. The confocal immunofluorescence images demonstrated that the D<sub>1</sub>R and D<sub>5</sub>R were both highly expressed in the proximal tubule and showed a similar sub-cellular localization, i.e., sub-apical position at the base of the microvilli (Figure S2). The composite images of both human and rat tubules demonstrated extensive co-localization in the sub-apical region. This sub-apical localization of the two receptors was verified by co-staining with a sub-apical marker α-adaptin (data not shown).

FRET analysis of these experiments was not possible because the two antibodies that work well on fixed tissue bind to either intracellular (D<sub>1</sub>R) or extracellular (D<sub>5</sub>R) epitopes that are on opposite sides of the phospholipid bilayer and are therefore outside the distance measurable by FRET. We therefore investigated their possible heterooligomerization using live-FRET microscopy. Figure S3 demonstrates live-cell sensitized emission-corrected FRET analysis of two different color-GFP fusion proteins of D<sub>1</sub>R and D<sub>5</sub>R heterologously expressed in HEK293 cells. A positive corrected FRET signal suggests that the two receptors are within 10 nm of each other. We verified these findings in lightly fixed non-permeabilized human RPTCs (Figure 2), using two different extracellular epitope-specific fluorescently-labeled antibodies that should bind to both epitopes either on the D<sub>1</sub>R or the D<sub>5</sub>R. These two antibodies should be found on the same side of the phospholipid bilayer and therefore can be used for FRET analysis. The photomicrographs in Figure 2 demonstrated a clear cell surface FRET signal. The addition of FEN (1 μmol/L, 30-min) increased the FRET signal and the amount of D<sub>1</sub>R at the cell surface.

A new D<sub>5</sub>R antagonist (LE-PM436)<sup>28</sup> was utilized to distinguish signaling of D<sub>5</sub>R from D<sub>1</sub>R. To validate its selectivity, we used HEK293 cells that were stably transfected with either D<sub>1</sub>R or D<sub>5</sub>R cDNA and expressed these receptors at normal physiological concentrations, measured at 3 pmoles/mg membrane protein.<sup>29</sup> cAMP production was measured following SKF38393 (non-selective D<sub>1</sub>R/D<sub>5</sub>R receptor agonist, 1 μmol/L, 30-min) stimulation and blocked with LE300 (non-selective D<sub>1</sub>R/D<sub>5</sub>R receptor antagonist) and LE-PM436 (selective D<sub>5</sub>R antagonist) (Figure 3). The addition of LE300 (10 μmol/L) inhibited SKF-stimulated intracellular cAMP production in both D<sub>1</sub>R and D<sub>5</sub>R-expressing HEK293 cells, confirming that it is not selective to either D<sub>1</sub>R or D<sub>5</sub>R. LE-PM436 (1 nmol/L)

inhibited SKF-stimulated cAMP production by  $84.0 \pm 1.2\%$  in D<sub>5</sub>R-expressing HEK293 cells, but did not inhibit the SKF-stimulated cAMP production in D<sub>1</sub>R-expressing HEK293 cells, confirming that LE-PM436 is a D<sub>5</sub>R-selective antagonist ( $P < 0.001$  vs SKF+VEH, N=8 per group). These studies also confirm the coupling of either D<sub>1</sub>R or D<sub>5</sub>R to AC, however the amount of cAMP produced by D<sub>5</sub>R-transfected HEK293 cells in response to SKF was  $26.4 \pm 0.5\%$  the amount measured from the D<sub>1</sub>R-transfected cells (N=18,  $P < 0.001$ , data not shown), despite similar receptor expression (using Bodipy630 SKF83566 binding, N=12, data not shown). Basal cAMP levels were  $1.04 \pm 0.08$  pmoles/mg protein in D<sub>1</sub>R-expressing HEK293 cells, and  $1.13 \pm 0.03$  pmoles/mg protein in D<sub>5</sub>R-expressing HEK293 cells. Induced levels for D<sub>1</sub>R-expressing HEK293 cells were  $15.52 \pm 1.07$  pmoles/mg protein following SKF exposure (30-min, 1  $\mu\text{mol/L}$ ) and induced levels of D<sub>5</sub>R-expressing HEK293 cells were  $4.01 \pm 0.08$  pmoles/mg protein.

Intracellular calcium, cAMP, and PLC levels were measured in RPTCs in response to FEN with and without the antagonists LE300 (D<sub>1</sub>R and D<sub>5</sub>R), U73122 (PLC) and LE-PM436 (D<sub>5</sub>R) (Figure 4). The left Y-axis depicts the ICUE3 (measure of intracellular cAMP accumulation) and CYPHR (measure of intracellular PLC activation state), normalized to vehicle (VEH). The right Y-axis depicts the intracellular ratiometric Ca<sup>++</sup> concentration measured by FURA-2. Stimulation with FEN (1  $\mu\text{mol/L}$ , 20-min) increased the cAMP levels, PLC activity, and Ca<sup>++</sup> levels in RPTCs ( $\#P < 0.001$  vs VEH, N=6 for ICUE3/CYPHR, N=11 for FURA-2). The addition of the D<sub>1</sub>R/D<sub>5</sub>R antagonist LE300 (10  $\mu\text{mol/L}$ , 20-min) blocked the FEN-mediated increase of all 3 variables ( $*P < 0.001$  vs FEN, N=6 for ICUE3/CYPHR, N=17 for FURA-2). Both the PLC inhibitor U73122 (10  $\mu\text{mol/L}$ , 20 min) and the D<sub>5</sub>R-specific inhibitor LE-PM436 (1 nmol/L, 20-min) blocked the FEN-mediated PLC activation but did not affect cAMP levels ( $*P < 0.001$  vs FEN, N=3-14). The D<sub>1</sub>R/D<sub>5</sub>R receptor AC-specific activator SKF83822 (10  $\mu\text{mol/L}$ , 20-min) caused an increase only in cAMP levels and not Ca<sup>++</sup> levels or PLC activity ( $\#P < 0.001$  vs VEH, N=3-17). By contrast, the PLC-activator SKF83959 (10  $\mu\text{mol/L}$ , 20-min) increased PLC activity and Ca<sup>++</sup> levels but not cAMP ( $\#P < 0.001$  vs VEH, N=4-17) levels. When these two agonists (SKF83822 and SKF83959) were combined there was no additive effect (data not shown).

We next utilized siRNA technology. The efficacy of the siRNA is demonstrated in Figure S4, using immunofluorescence staining of transfected RPTCs. RPTCs that were transfected with D<sub>1</sub>R or D<sub>5</sub>R siRNA had a marked decrease in their respective expression levels compared to scrambled (SCR) RNA control, using the same timing and format as the sodium assays ( $P < 0.001$  vs SCR, N=4). Figure 5 shows that D<sub>1</sub>R siRNA blocked the FEN-stimulated increase in cAMP accumulation and PLC activity ( $*P < 0.05$  vs SCR, N=16 for ICUE3, N=4 for CYPHR). By contrast, the D<sub>5</sub>R siRNA blocked only the FEN-mediated increase in PLC activity ( $*P < 0.05$  vs SCR, N=4), while the combination of the D<sub>1</sub>R and D<sub>5</sub>R siRNAs blocked both signaling pathways ( $*P < 0.05$  vs SCR, N=14 for ICUE3, N=4 for CYPHR). These data indicate that in RPTCs, the D<sub>1</sub>R is coupled to both AC and PLC whereas the D<sub>5</sub>R is linked mainly to PLC. This is in contrast to the linkage of D<sub>5</sub>R to AC in HEK293 cells heterologously expressing D<sub>5</sub>R.

We next determined how selective D<sub>1</sub>R and/or D<sub>5</sub>R stimulation or reduction with siRNA would ultimately affect sodium influx via NHE3 or sodium efflux via NaKATPase (Figure

6). The D<sub>1</sub>R/D<sub>5</sub>R agonist FEN (1 μmol/L, 30-min) inhibited both NHE3-mediated sodium influx and NaKATPase-mediated sodium efflux in immortalized RPTCs (\*P<0.0001 vs VEH, N=6, Figure 6, Panel A). The addition of U73122 (10 μmol/L), LE-PM436 (1 nmol/L), or LE300 (10 μmol/L), by themselves did not affect sodium influx or efflux (data not shown) but their co-incubation with FEN returned the sodium influx and efflux to VEH levels. The D<sub>1</sub>-like receptor AC-specific activator SKF83822 (10 μmol/L, 20-min) inhibited both NHE3 and NaKATPase (#P<0.001 vs VEH, N=6). By contrast, the PLC-activator SKF83959 (10 μmol/L, 20-min) did not inhibit either NHE3 or NaKATPase activity. This suggests that the primary inhibitory signaling pathway for NHE3 and NaKATPase is via AC. The combination of SKF83822 and SKF83959 inhibited both NHE3 and NaKATPase (\*P<0.0001 vs VEH, N=6), and to a greater extent than SKF83822 alone. As shown in Figure 6 (Panel B), the FEN-mediated inhibition of sodium influx and efflux were reversed by siRNA specific to D<sub>1</sub>R, D<sub>5</sub>R, or both D<sub>1</sub>R and D<sub>5</sub>R (\*P<0.05 vs SCR, \*\*P<0.001 vs SCR, N=6). These data indicate that both the cAMP and PLC pathways are necessary for inhibition of sodium influx and efflux, involving both D<sub>1</sub>R and D<sub>5</sub>R.

In order to control for the effects of the antagonists alone (U73122, LE-PM436 and LE300), each one was included in both the sodium influx and efflux assays and showed no effect in either assay (data not shown). Antisense oligos to the D<sub>1</sub>R or D<sub>5</sub>R<sup>20</sup> recapitulated the effects we observed with the specific inhibitors of either D<sub>1</sub>R or D<sub>5</sub>R (data not shown).

## Discussion

The interplay between the D<sub>1</sub>R and D<sub>5</sub>R, two closely related cell surface receptors that share the same endogenous agonist (dopamine), is important in understanding the role of dopamine in cell function. The D<sub>1</sub>R and D<sub>5</sub>R are expressed in different areas of the brain, which suggests that the D<sub>5</sub>R has a distinct role in neurotransmission when compared to the D<sub>1</sub>R.<sup>16</sup> However, the direct interaction of endogenously expressed D<sub>1</sub>R and D<sub>5</sub>R has not been well studied. Dopamine receptors outside the central nervous system are often expressed within the same cells. For example, the D<sub>1</sub>R and D<sub>5</sub>R are both expressed in the tunica media of systemic arteries<sup>30</sup> and both are expressed in almost all segments of the nephron where active sodium transport occurs.<sup>17</sup> D<sub>1</sub>R and D<sub>5</sub>R heterologously co-expressed in HEK293 cells have been found to hetero-oligomerize.<sup>31</sup>

In our current studies, we demonstrated that the D<sub>1</sub>R and D<sub>5</sub>R were not only present in RPTCs, but they co-localized, co-immunoprecipitated, and directly physically interacted, as demonstrated by FRET microscopy. The co-localization of the D<sub>1</sub>R and D<sub>5</sub>R was seen in a compartment at the base of the microvilli in the proximal tubule in human and rat kidneys. Microvilli are key structures in the renal proximal tubule that serve to increase the luminal membrane surface area for protein and peptide uptake and catabolism and ion transport. Microvilli also serve as sensors for sampling and adjusting the concentration of various solutes within the glomerular filtrate in response to mechanotransduction.<sup>32</sup> The D<sub>5</sub>R and D<sub>1</sub>R were found clustered in a tight band in the sub-microvilliary space, where they could be rapidly recruited to the plasma membrane in response to cell surface receptor stimulation. We demonstrated in the current report that the D<sub>1</sub>R/D<sub>5</sub>R agonist FEN caused recruitment of

the D<sub>1</sub>R to the cell surface plasma membrane, corroborating our previous report using surface biotinylation and western blot analysis.<sup>33</sup>

We have reported that salt-sensitive hypertension in humans correlates with defective recruitment of D<sub>1</sub>R to the cell surface of urinary RPTCs when their intracellular sodium levels were increased.<sup>34</sup> In contrast, we found that the D<sub>5</sub>R was not recruited to the cell surface but appears to have a constant cell membrane concentration not altered by agonist stimulation.<sup>35</sup> We further found that this constant level of D<sub>5</sub>R at the cell membrane was lower in RPTCs whose D<sub>1</sub>R coupling to AC was defective.<sup>35</sup> The D<sub>5</sub>R has not been demonstrated to stimulate cAMP accumulation in the kidney but has been shown to couple to AC in heterologous overexpression systems such as the HEK293 cells shown in this report. Overexpression of proteins can result in promiscuous associations and therefore, we studied D<sub>1</sub>R and D<sub>5</sub>R endogenously expressed in the same cell, i.e., RPTC. These studies are the first demonstration of the blocking of cellular D<sub>5</sub>R-coupled second messenger activity using a selective D<sub>5</sub>R antagonist, LE-PM436 and siRNA to the D<sub>5</sub>R demonstrated similar blocking effects in all experimental assays further confirming the selectivity of LE-PM436 to the D<sub>5</sub>R. However, LE-PM436 may have an important advantage over siRNA in studying the D<sub>5</sub>R because the long-term silencing of the D<sub>5</sub>R expression by siRNA cannot be readily reversed. Our current studies showed for the first time in RPTCs that endogenously express both D<sub>1</sub>R and D<sub>5</sub>R that the D<sub>5</sub>R preferentially stimulated PLC activity and increased intracellular Ca<sup>++</sup>, effects that were inhibited by the D<sub>5</sub>R selective antagonist LE-PM436. The independence of these pathways is highlighted by the data that demonstrated that SKF83822 stimulated AC but not PLC, while SKF83959 stimulated PLC but not AC. Also, neither SKF83822 nor SKF83959 inhibited the pathway that it does not stimulate. This distinction is important because there is a PKA and PKC cross-talk following D<sub>1</sub>R<sup>36</sup> and D<sub>1</sub>-like receptor<sup>37</sup> stimulation. Indeed in the current study, PLC stimulation was blocked when the D<sub>1</sub>R was silenced. It has been shown that dopaminergic inhibition of NaKATPase via PLC and PKC is Na<sup>+</sup> dependent.<sup>38</sup>

Previous reports have demonstrated that D<sub>1</sub>-like receptor stimulation inhibited various ion transporters and exchangers in the renal proximal tubule luminal membrane (NHE3, Na<sup>+</sup>Pi co-transporter, and the Cl<sup>-</sup>/HCO<sub>3</sub><sup>-</sup> exchanger) and ion exchanger and sodium pump in the basolateral membrane (NaKATPase, and the Cl<sup>-</sup>/HCO<sub>3</sub><sup>-</sup> exchanger).<sup>26</sup> However, it is not known which D<sub>1</sub>-like receptor subtype, D<sub>1</sub>R or D<sub>5</sub>R, mediates these effects. In D<sub>5</sub>R deficient mice, distal tubular sodium transporters/channels (Na<sup>+</sup>K<sup>+</sup>2Cl<sup>-</sup> co-transporter, Na<sup>+</sup>Cl<sup>-</sup> co-transporter, and the  $\alpha$  and  $\gamma$  subunits of the epithelial sodium channel) were increased,<sup>39</sup> suggesting a tonic inhibition of the activity of these proteins via the D<sub>5</sub>R. In the current experiments, we showed that in addition to a functional D<sub>1</sub>R, D<sub>5</sub>R stimulation was also necessary for the inhibition of NHE3-mediated sodium influx and NaKATPase-mediated sodium efflux following D<sub>1</sub>R/D<sub>5</sub>R receptor stimulation. Taken together with our previous studies demonstrating that the D<sub>5</sub>R is responsible for the tonic down-regulation of the anti-natriuretic angiotensin II type 1 receptor (AT<sub>1</sub>R) in rat and human RPTCs, these data suggest that the D<sub>1</sub>R is the mediator, while the D<sub>5</sub>R as part of the D<sub>1</sub>R/D<sub>5</sub>R heteromer and PLC signaling acts as the modulator, of the inhibition of sodium transport. Our proposed model for these pathways and their roles in sodium transport (NHE3 and NaKATPase) regulation is shown in Figure 7.

Previous studies on the physiological effects of dopamine and synthetic dopamine agonists and antagonists have been confounded by the lack of a selective antagonist to either receptor. The recent availability of LE-PM436 will now enable the *in vivo* study of the selective roles of the renal D<sub>1</sub>R and D<sub>5</sub>R receptors. An overactive renal renin angiotensin system (RAS) and diminished function of the renal dopaminergic system has been associated with hypertension and salt-sensitivity *in-vivo* in mouse, rats, and humans.<sup>40</sup> One class of anti-hypertensive pharmaceutical drugs that affect these systems and consequently blood pressure in all three species are AT<sub>1</sub>R blockers. One of the many beneficial effects of AT<sub>1</sub>R blockers may be mediated through the pathways described in this paper. Higher expression of angiotensinogen in high salt conditions, as well as numerous SNPs in the RAS system such as ACE, angiotensinogen or AT<sub>1</sub>R, could lead to overactive AT<sub>1</sub>R stimulation, downregulation of the D<sub>5</sub>R and subsequent loss of D<sub>5</sub>R-PLC specific natriuresis.<sup>41</sup> Use of AT<sub>1</sub>R blockers under high salt conditions would allow the increased conversion of L-dopa to dopamine in the proximal tubule to stimulate both the D<sub>1</sub>R and D<sub>5</sub>R to aid in natriuresis and lower blood pressure since there would be diminished counter-regulation by the AT<sub>1</sub>R. The implications of this paper may also suggest reasons why AT<sub>1</sub>R blockers are not always effective; patients with proximal tubule D<sub>1</sub>R -AC uncoupling may have diminished high salt D<sub>5</sub>R-PLC induction of natriuresis. In animal models, the drug LE-PM436 would allow testing of these hypotheses in acute studies that otherwise would be difficult with siRNA or knockout models where gene compensation could alter the proper interpretation of the results.

## Methods

### RPTC Culture

RPTCs were obtained from normal tissue from nephrectomies in human subjects, under an institutional review board-approved protocol according to the Declaration of Helsinki, Title 45, Part 46, and U.S. Code of Federal Regulations. Cell lines were immortalized as previously described<sup>33, 42, 43</sup> and demonstrated only proximal tubule-specific characteristics as extensively detailed in our previous publication.<sup>27</sup> We have identified two distinct subpopulations of RPTCs, those that have a D<sub>1</sub>R with normal AC coupling, and those with defective D<sub>1</sub>R to AC coupling (uncoupled). We utilized only the normally-coupled RPTC lines i7448, i16, and i22 in the current studies, since a fully functional D<sub>1</sub>R is necessary in our sodium transport assays.<sup>27</sup>

### HEK293 Cell Culture and Transfection

Human embryonic kidney (HEK293) cells were obtained from ATCC (Manassas, VA) and grown in DMEM high glucose with 10% FBS. They were stably transfected with human D<sub>1</sub>R and D<sub>5</sub>R as previously described<sup>23, 44</sup> and these cells were used to confirm the specificity of LE-PM436 for the D<sub>5</sub>R. For transient transfection of GFP fusion constructs used in the live FRET analysis, the D<sub>1</sub>R and the D<sub>5</sub>R were PCR-amplified from cDNA clones obtained from the Missouri S&T cDNA Resource Center ([www.cdna.org](http://www.cdna.org)) and subcloned into the pEGFP-N1 vector (Clontech) that had the EGFP replaced with either CyPet for D<sub>5</sub>R or YPet for D<sub>1</sub>R.

## Pharmacological Agents

The D<sub>1</sub>-like (D<sub>1</sub>R/D<sub>5</sub>R) receptor agonists, FEN and SKF38393, were used along with D<sub>1</sub>-like (D<sub>1</sub>R/D<sub>5</sub>R) receptor antagonist LE300 and the novel selective D<sub>5</sub>R antagonist LE-PM436. PLC inhibitor U73122, cAMP-specific activator SKF83822, and PLC-specific activator SKF83959 were also used. Details about these and the ouabain and EIPA used in the sodium transport assays (including source information) can be found in Table S1 in the Online Supplement.

## Co-Immunoprecipitation of D<sub>1</sub>R and D<sub>5</sub>R

Co-immunoprecipitation of the two receptors was performed as previously described<sup>33</sup> using rabbit D<sub>1</sub>R antibody (1:50 dilution, sc-14001, Santa Cruz Biotechnology). The detection step used goat polyclonal anti-D<sub>5</sub>R (1:100 dilution, sc-1440 Santa Cruz Biotechnology), followed by a donkey anti-goat IR Dye 800 secondary antibody (1:15,000, LI-COR Biosciences). Non-specific rabbit IgG (Sigma) was used as a negative control immunoprecipitating antibody and no D<sub>5</sub>R-specific signal was detected. Lack of cross reactivity with the respective antibodies was verified using the stably transfected D<sub>1</sub>R-HEK293 and D<sub>5</sub>R-HEK293 cells. The FEN effect was measured after 30-min (1 μmol/L FEN).

## Immunofluorescence

The basic immunofluorescent staining procedure has been reported.<sup>27</sup> The D<sub>1</sub>R antibody used on fixed tissue was from Dr. Jose's laboratory.<sup>45</sup> The 3<sup>rd</sup> extracellular loop-specific D<sub>1</sub>R antibody used for cell surface labeling was from Dr. Carey's laboratory.<sup>46,47</sup> The 3<sup>rd</sup> extracellular loop-specific D<sub>5</sub>R antibody used in fixed tissue and for cell surface labeling was from Millipore (AB 9509). Details about both staining procedures are in the Online Supplement.

## Sensitized Emission FRET Microscopy

Sensitized emission Fluorescent Resonance Energy Transfer (FRET) analysis of the physical association of D<sub>1</sub>R and D<sub>5</sub>R was performed using two different systems. One system utilized live-cell microscopy of HEK293 cells transiently transfected with D<sub>1</sub>R-YPet (yellow fluorescent protein) and D<sub>5</sub>R-CyPet (cyan fluorescent protein) fluorescent protein fusion constructs. The second set of experiments was performed on fixed non-permeabilized RPTCs using extracellular epitope-specific and directly-fluorescently-labeled antibodies to the D<sub>1</sub>R and D<sub>5</sub>R using Alexa 488 and Alexa 555 dyes, respectively. Live-cell imaging was performed using a Biopetechs Delta T stage heating system and Biopetechs objective heater. Spectral bleedthrough calculations and corrected FRET (cFRET) imaging was performed according to the FRET Module of Slidebook 4.2. Verification of proper microscope setup and calculations was provided by using both positive (ICUE3 FRET biosensor for CyPet/YPet and ICUE-YR for 488/555) and negative controls (co-transfected CyPet and YPet non-fusion fluorescent proteins). Details about filters and FRET analysis are in the Online Supplement.



### Fluorescent Biosensors for cAMP Accumulation (ICUE3) and PLC Activation (CYPHR)

cAMP accumulation and PLC activation were measured by intracellular real-time kinetic assays using the fluorescent biosensors ICUE3 and CYPHR, respectively. This involved transfecting RPTCs with a plasmid containing a novel fluorescence resonance energy transfer sensor for cAMP (ICUE3) or Addgene plasmid 14864 for PLC activation (CYPHR) according to the methods of Violin et al.<sup>48,49</sup>

The ICUE biosensor contains a cAMP binding domain of EPAC1, a known cAMP target in proximal tubule cells necessary for NHE3 inhibition.<sup>50</sup> RPTCs were electroporated according to our previously optimized protocol.<sup>33</sup> They were allowed to recover in culture media for 24-hr before imaging. Cells were treated with combinations of agonists and antagonists and imaged with confocal microscopy every 30 sec for 20-min. The final read was used to generate the data in Figures 4 and 5.

### siRNA

100 nmol/L D<sub>1</sub>R siRNA (target sequence: 5' CAUCUCAUCCUCUGUAAUA 3'), D<sub>1</sub>R scrambled control (5' GCAUCUUUACACCACUUUAU 3'), D<sub>5</sub>R siRNA (target sequence: 5' CCCUUCUUCAUCCUUAACU 3') or D<sub>5</sub>R scrambled control (5' CUCCAUUCUCCAUCUUCUAU 3') was transfected for 24-hr into RPTCs by electroporation as previously published.<sup>33</sup>

### NHE3-mediated Sodium Influx Assay

Details and specificity of this assay, where we use ouabain to inhibit NaKATPase and measure sodium accumulation in RPTCs, was previously published<sup>27</sup> and is described in the Online Supplement. The figures were made using data collected at the 30-min time point.

### NaKATPase-mediated Sodium Efflux Assay

The detailed method used to measure the rate of sodium efflux was previously published<sup>33</sup> and is outlined in the Online Supplement. The figures were made using data collected at the 30-min time point.

### Calcium Imaging

RPTCs were labeled with fura-2 AM (Invitrogen) using identical conditions established for the SBFI labeling as stated in the NHE3-mediated sodium influx assay. The fura-2 here simply replaces the SBFI used in the influx assay. The filter set and imaging parameters are also identical for the two assays. Data for this figure was collected at the 20-min time point.

### cAMP Assay

cAMP accumulation was measured after 30-min of agonist stimulation (SKF38393, see Table S1) with IBMX (500 μmol/L) using a commercial ELISA kit (Cayman Chemical) as previously described.<sup>33</sup> Antagonists LE-PM436 and LE300 (see Table S1) were added 10-min prior to the agonist incubation.

## Statistical Analysis

The data are expressed as mean  $\pm$  SE. Comparisons within and among groups were made by repeated measures or factorial ANOVA, respectively, followed by Holm-Sidak or Duncan's test. Student's t-test was used for two-group comparisons. P values of  $<0.05$  were considered significant.

## Supplementary Material

Refer to Web version on PubMed Central for supplementary material.

## Acknowledgments

**Sources of Funding:** This work was funded by National Institutes of Health grants HL023081, HL092196, HL074940, DK039308.

## References

1. Siragy HM, Felder RA, Howell NL, et al. Evidence that intrarenal dopamine acts as a paracrine substance at the renal tubule. *Am J Physiol.* 1989; 257:F469–477. [PubMed: 2528916]
2. Pelayo JC, Fildes RD, Eisner GM, et al. Effects of dopamine blockade on renal sodium excretion. *Am J Physiol.* 1983; 245:F247–253. [PubMed: 6881340]
3. Jose PA, Eisner GM, Felder RA. Dopamine and the kidney: a role in hypertension? *Curr Opin Nephrol Hypertens.* 2003; 12:189–194. [PubMed: 12589180]
4. Hussain T, Lokhandwala MF. Renal dopamine receptors and hypertension. *Exp Biol Med (Maywood).* 2003; 228:134–142. [PubMed: 12563019]
5. Jose PA, Eisner GM, Felder RA. Renal dopamine receptors in health and hypertension. *Pharmacol Ther.* 1998; 80:149–182. [PubMed: 9839770]
6. Zhang MZ, Yao B, Wang S, et al. Intrarenal dopamine deficiency leads to hypertension and decreased longevity in mice. *J Clin Invest.* 2011; 121:2845–2854. [PubMed: 21701066]
7. Sunahara RK, Guan HC, O'Dowd BF, et al. Cloning of the gene for a human dopamine D5 receptor with higher affinity for dopamine than D1. *Nature.* 1991; 350:614–619. [PubMed: 1826762]
8. Kimura K, White BH, Sidhu A. Coupling of human D-1 dopamine receptors to different guanine nucleotide binding proteins. Evidence that D-1 dopamine receptors can couple to both Gs and G(o). *J Biol Chem.* 1995; 270:14672–14678. [PubMed: 7782330]
9. Corvol JC, Studler JM, Schonn JS, et al. Galpha(olf) is necessary for coupling D1 and A2a receptors to adenylyl cyclase in the striatum. *J Neurochem.* 2001; 76:1585–1588. [PubMed: 11238742]
10. Sidhu A, Kimura K, Uh M, et al. Multiple coupling of human D5 dopamine receptors to guanine nucleotide binding proteins Gs and Gz. *J Neurochem.* 1998; 70:2459–2467. [PubMed: 9603210]
11. Zheng S, Yu P, Zeng C, et al. Galpha12- and Galpha13-protein subunit linkage of D5 dopamine receptors in the nephron. *Hypertension.* 2003; 41:604–610. [PubMed: 12623966]
12. Jin LQ, Wang HY, Friedman E. Stimulated D(1) dopamine receptors couple to multiple Galpha proteins in different brain regions. *J Neurochem.* 2001; 78:981–990. [PubMed: 11553672]
13. Jin LQ, Goswami S, Cai G, et al. SKF83959 selectively regulates phosphatidylinositol-linked D1 dopamine receptors in rat brain. *J Neurochem.* 2003; 85:378–386. [PubMed: 12675914]
14. Sahu A, Tyeryar KR, Vongtau HO, et al. D5 dopamine receptors are required for dopaminergic activation of phospholipase C. *Mol Pharmacol.* 2009; 75:447–453. [PubMed: 19047479]
15. Undieh AS. Pharmacology of signaling induced by dopamine D(1)-like receptor activation. *Pharmacol Ther.* 2010; 128:37–60. [PubMed: 20547182]
16. Ciliax BJ, Nash N, Heilman C, et al. Dopamine D(5) receptor immunolocalization in rat and monkey brain. *Synapse.* 2000; 37:125–145. [PubMed: 10881034]

17. Zeng C, Armando I, Luo Y, et al. Dysregulation of dopamine-dependent mechanisms as a determinant of hypertension: studies in dopamine receptor knockout mice. *Am J Physiol Heart Circ Physiol*. 2008; 294:H551–569. [PubMed: 18083900]
18. Felder CC, Jose PA, Axelrod J. The dopamine-1 agonist, SKF 82526, stimulates phospholipase-C activity independent of adenylate cyclase. *J Pharmacol Exp Ther*. 1989; 248:171–175. [PubMed: 2563286]
19. Vyas SJ, Jadhav AL, Eichberg J, et al. Dopamine receptor-mediated activation of phospholipase C is associated with natriuresis during high salt intake. *Am J Physiol*. 1992; 262:F494–498. [PubMed: 1558166]
20. Gildea JJ, Wang X, Jose PA, et al. Differential D1 and D5 receptor regulation and degradation of the angiotensin type 1 receptor. *Hypertension*. 2008; 51:360–366. [PubMed: 18172057]
21. Albrecht FE, Drago J, Felder RA, et al. Role of the D1A dopamine receptor in the pathogenesis of genetic hypertension. *J Clin Invest*. 1996; 97:2283–2288. [PubMed: 8636408]
22. Hollon TR, Bek MJ, Lachowicz JE, et al. Mice lacking D5 dopamine receptors have increased sympathetic tone and are hypertensive. *J Neurosci*. 2002; 22:10801–10810. [PubMed: 12486173]
23. Yang Z, Asico LD, Yu P, et al. D5 dopamine receptor regulation of reactive oxygen species production, NADPH oxidase, and blood pressure. *Am J Physiol Regul Integr Comp Physiol*. 2006; 290:R96–R104. [PubMed: 16352863]
24. Yang Z, Sibley DR, Jose PA. D5 dopamine receptor knockout mice and hypertension. *J Recept Signal Transduct Res*. 2004; 24:149–164. [PubMed: 15521360]
25. Yang Z, Asico LD, Yu P, et al. D5 dopamine receptor regulation of reactive oxygen species production, NADPH oxidase, and blood pressure. *American Journal of Physiology - Regulatory Integrative & Comparative Physiology*. 2006; 290:R96–R104.
26. Zeng C, Yang Z, Asico LD, et al. Regulation of blood pressure by D5 dopamine receptors. *Cardiovasc Hematol Agents Med Chem*. 2007; 5:241–248. [PubMed: 17630951]
27. Gildea JJ, Shah I, Weiss R, et al. HK-2 human renal proximal tubule cells as a model for G protein-coupled receptor kinase type 4-mediated dopamine 1 receptor uncoupling. *Hypertension*. 2010; 56:505–511. [PubMed: 20660820]
28. Mohr P, Decker M, Enzensperger C, et al. Dopamine/serotonin receptor ligands. 12(1): SAR studies on hexahydro-dibenz[d,g]azecines lead to 4-chloro-7-methyl-5,6,7,8,9,14-hexahydrodibenz[d,g]azecin-3-ol, the first picomolar D5-selective dopamine-receptor antagonist. *J Med Chem*. 2006; 49:2110–2116. [PubMed: 16539400]
29. Yu P, Yang Z, Jones JE, et al. D1 dopamine receptor signaling involves caveolin-2 in HEK-293 cells. *Kidney international*. 2004; 66:2167–2180. [PubMed: 15569306]
30. Amenta F, Ricci A, Tayebati SK, et al. The peripheral dopaminergic system: morphological analysis, functional and clinical applications. *Ital J Anat Embryol*. 2002; 107:145–167. [PubMed: 12437142]
31. O'Dowd BF, Ji X, Alijaniam M, et al. Dopamine receptor oligomerization visualized in living cells. *J Biol Chem*. 2005; 280:37225–37235. [PubMed: 16115864]
32. Weinbaum S, Duan Y, Satlin LM, et al. Mechanotransduction in the renal tubule. *Am J Physiol Renal Physiol*. 2010; 299:F1220–1236. [PubMed: 20810611]
33. Gildea JJ, Israel JA, Johnson AK, et al. Caveolin-1 and dopamine-mediated internalization of NaKATPase in human renal proximal tubule cells. *Hypertension*. 2009; 54:1070–1076. [PubMed: 19752292]
34. Gildea JJ, Lahiff DT, Van Sciver RE, et al. A linear relationship between the ex-vivo sodium mediated expression of two sodium regulatory pathways as a surrogate marker of salt sensitivity of blood pressure in exfoliated human renal proximal tubule cells: the virtual renal biopsy. *Clin Chim Acta*. 2013; 421:236–242. [PubMed: 23454474]
35. Gildea JJ, Wang X, Shah N, et al. Dopamine and Angiotensin type 2 receptors cooperatively inhibit sodium transport in human renal proximal tubule cells. *Hypertension*. 2012; 60:396–403. [PubMed: 22710646]
36. Yu P, Han W, Villar VA, et al. Dopamine D1 receptor-mediated inhibition of NADPH oxidase activity in human kidney cells occurs via protein kinase A-protein kinase C cross talk. *Free Radic Biol Med*. 2011; 50:832–840. [PubMed: 21193028]

37. Gomes P, Soares-da-Silva P. Role of cAMP-PKA-PLC signaling cascade on dopamine-induced PKC-mediated inhibition of renal Na(+)-K(+)-ATPase activity. *Am J Physiol Renal Physiol.* 2002; 282:F1084–1096. [PubMed: 11997325]
38. Efendiev R, Budu CE, Cinelli AR, et al. Intracellular Na<sup>+</sup> regulates dopamine and angiotensin II receptors availability at the plasma membrane and their cellular responses in renal epithelia. *J Biol Chem.* 2003; 278:28719–28726. [PubMed: 12759348]
39. Wang X, Luo Y, Escano CS, et al. Upregulation of renal sodium transporters in D5 dopamine receptor-deficient mice. *Hypertension.* 2010; 55:1431–1437. [PubMed: 20404220]
40. Armando I, Villar VA, Jose PA. Dopamine and renal function and blood pressure regulation. *Compr Physiol.* 2011; 1:1075–1117. [PubMed: 23733636]
41. Gildea JJ. Dopamine and angiotensin as renal counterregulatory systems controlling sodium balance. *Curr Opin Nephrol Hypertens.* 2009; 18:28–32. [PubMed: 19077686]
42. Felder RA, Sanada H, Xu J, et al. G protein-coupled receptor kinase 4 gene variants in human essential hypertension. *Proc Natl Acad Sci USA.* 2002; 99:3872–3877. [PubMed: 11904438]
43. Sanada H, Jose PA, Hazen-Martin D, et al. Dopamine-1 receptor coupling defect in renal proximal tubule cells in hypertension. *Hypertension.* 1999; 33:1036–1042. [PubMed: 10205244]
44. Yu P, Yang Z, Jones JE, et al. D1 dopamine receptor signaling involves caveolin-2 in HEK-293 cells. *Kidney Int.* 2004; 66:2167–2180. [PubMed: 15569306]
45. Xu J, Li XX, Albrecht FE, et al. Dopamine(1) receptor, G(salpa), and Na(+)-H(+) exchanger interactions in the kidney in hypertension. *Hypertension.* 2000; 36:395–399. [PubMed: 10988271]
46. O'Connell DP, Botkin SJ, Ramos SI, et al. Localization of dopamine D1A receptor protein in rat kidneys. *Am J Physiol.* 1995; 268:F1185–1197. [PubMed: 7611459]
47. Brismar H, Asghar M, Carey RM, et al. Dopamine-induced recruitment of dopamine D1 receptors to the plasma membrane. *Proc Natl Acad Sci U S A.* 1998; 95:5573–5578. [PubMed: 9576924]
48. Violin JD, Zhang J, Tsien RY, et al. A genetically encoded fluorescent reporter reveals oscillatory phosphorylation by protein kinase C. *J Cell Biol.* 2003; 161:899–909. [PubMed: 12782683]
49. Violin JD, DiPilato LM, Yildirim N, et al. beta2-adrenergic receptor signaling and desensitization elucidated by quantitative modeling of real time cAMP dynamics. *J Biol Chem.* 2008; 283:2949–2961. [PubMed: 18045878]
50. Honegger KJ, Capuano P, Winter C, et al. Regulation of sodium-proton exchanger isoform 3 (NHE3) by PKA and exchange protein directly activated by cAMP (EPAC). *Proc Natl Acad Sci U S A.* 2006; 103:803–808. [PubMed: 16407144]

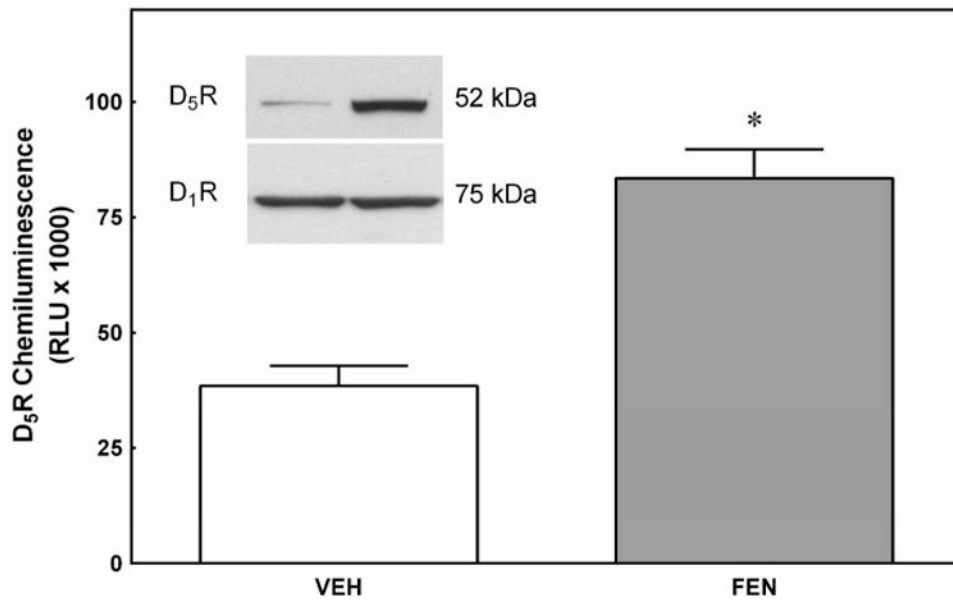


**Figure 1. Co-Immunoprecipitation of D<sub>1</sub>R and D<sub>5</sub>R**

Immortalized human RPTCs were incubated with and without fenoldopam (FEN, D<sub>1</sub>R/D<sub>5</sub>R agonist, 1  $\mu$ mol/L, 30 min) and the physical interaction between the D<sub>1</sub>R and D<sub>5</sub>R was determined by co-immunoprecipitation and western blotting. FEN induced an 111.7 $\pm$ 9.4% increase in D<sub>1</sub>R and D<sub>5</sub>R protein-protein interaction using a rabbit anti-D<sub>1</sub>R immunoprecipitating antibody and a goat anti-D<sub>5</sub>R detection antibody ( $P < 0.001$ ,  $N = 6$  per group).

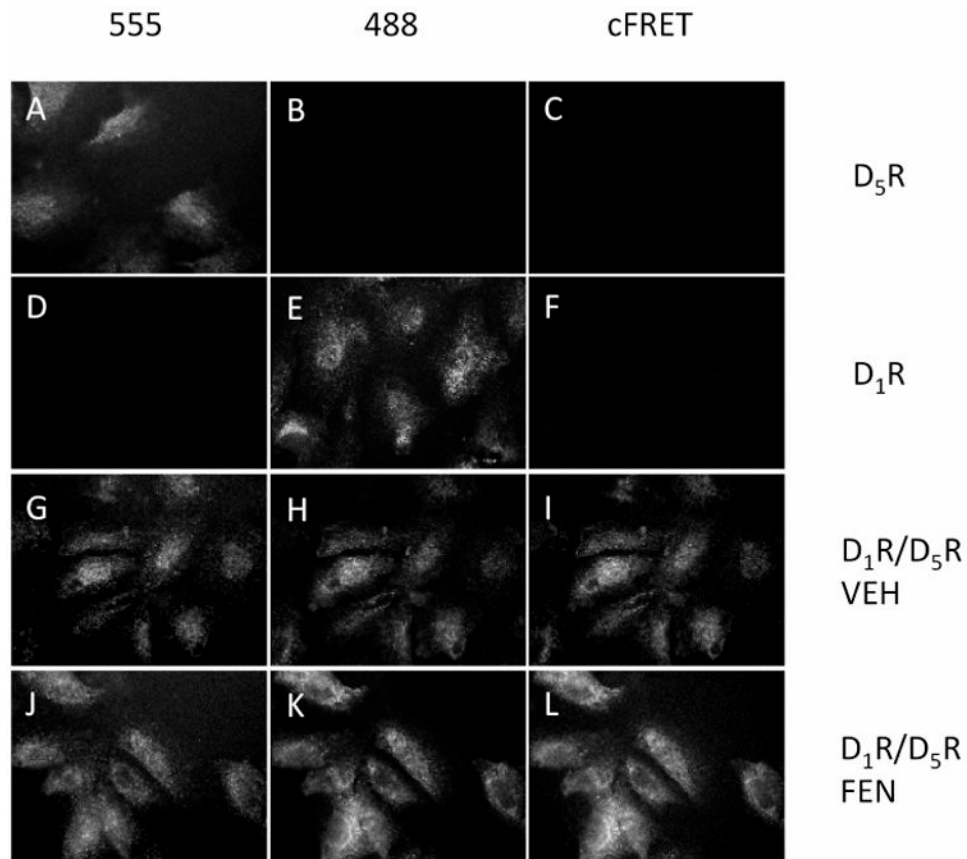


**Figure 2. Fixed cell surface D<sub>1</sub>R / D<sub>5</sub>R FRET measurement in non-permeabilized human RPTCs**  
 The first row of images indicates that when Alexa 555-labeled D<sub>5</sub>R antibody was added to the RPTCs, a clear signal was measured in the Alexa 555 channel (A), and there was no spectral bleedthrough into the Alexa 488 filter channel (B) and no measurable signal in the corrected FRET (cFRET) channel (C), as expected. The second row of images indicates that the same was true when the Alexa 488-labeled D<sub>1</sub>R antibody was added to RPTCs. There was a clear signal measured in the Alexa 488 channel (E), no spectral bleedthrough into the Alexa 555 channel (D) and no measurable signal in the cFRET channel (F). In the third row, RPTCs were first incubated with vehicle (VEH) and then with Alexa 555-labeled D<sub>5</sub>R and Alexa 488-labeled D<sub>1</sub>R antibodies. A clear signal was measured in the Alexa 555 (G) and Alexa 488 channels (H), and a clear cFRET signal was detected in the cFRET channel (I). In the bottom row, RPTCs were incubated with the D<sub>1</sub>R/D<sub>5</sub>R agonist fenoldopam (FEN, 1 μmol/L, 30 min) before fixing and staining with the two antibodies. An increase in the mean intensity of the Alexa 488 channel indicates that the D<sub>1</sub>R was recruited to the cell surface (K compared to H). Additionally there was an increase in cFRET signal upon addition of FEN (L compared to I). Images were collected using a 60× water immersion objective lens.

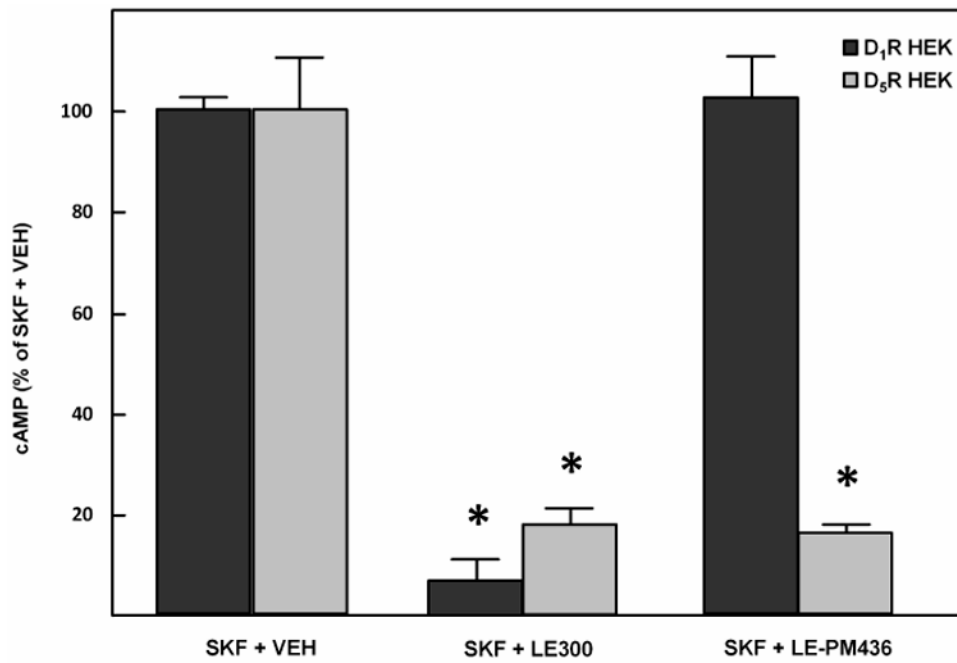


**Figure 3. Selective Inhibition of D<sub>5</sub>R-transfected HEK293 cells with LE-PM436**

The D<sub>1</sub>R/D<sub>5</sub>R antagonist LE300 (10  $\mu$ mol/L, 30 min) inhibited the stimulatory effect of SKF38393 (D<sub>1</sub>R/D<sub>5</sub>R agonist, 10  $\mu$ mol/L, 30 min) on intracellular cAMP production in both D<sub>1</sub>R- and D<sub>5</sub>R- transfected HEK293 cells. LE-PM436 (1 nmol/L, 30 min) only inhibited SKF-induced cAMP production in the D<sub>5</sub>R-transfected HEK293 cells (84.0  $\pm$  1.2% decrease, \*P<0.001 vs VEH, N=8 per group).

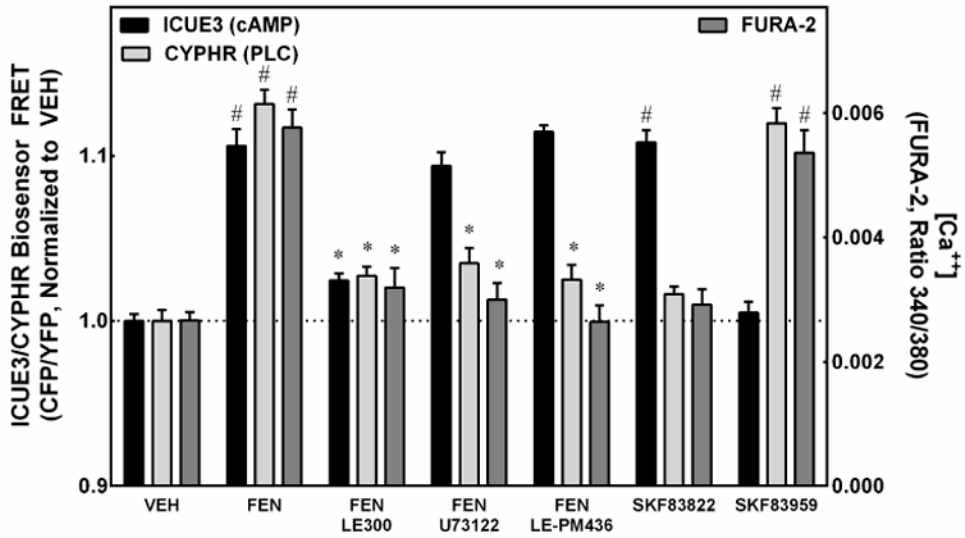


**Figure 4. D<sub>1</sub>R and D<sub>5</sub>R Specific Signaling to AC or PLC**

ICUE3 (measure of intracellular cAMP accumulation) and CYPHR (measure of intracellular PLC activation state) are depicted on the left Y-axis, normalized to vehicle (VEH). The right Y-axis depicts the intracellular Ca<sup>++</sup> using FURA-2. Stimulation with the D<sub>1</sub>R/D<sub>5</sub>R agonist fenoldopam (FEN, 1 μmol/L, 20 min) increased intracellular Ca<sup>++</sup> and cAMP levels and activated PLC (<sup>#</sup>P<0.001 vs VEH, N=6 for ICUE3/CYPHR, N=11 for FURA-2). Addition of the D<sub>1</sub>R/D<sub>5</sub>R antagonist LE300 (10 μmol/L, 20 min) blocked the FEN-mediated increase of all 3 variables (<sup>\*</sup>P<0.001 vs FEN, N=6 for ICUE3/CYPHR, N=17 for FURA-2). The PLC inhibitor U73122 (10 μmol/L, 20 min) and the D<sub>5</sub>R-specific inhibitor LE-PM436 (1 nmol/L, 20 min) both blocked the FEN-mediated increase in intracellular Ca<sup>++</sup> and PLC activity but did not affect cAMP levels (<sup>\*</sup>P<0.001 vs FEN, N=3-14). The AC-specific activator SKF83822 (10 μmol/L, 20 min) caused an increase only in cAMP (<sup>#</sup>P<0.001 vs VEH, N=3-17) and the PLC-specific activator SKF83959 (10 μmol/L, 20 min) increased PLC activity and Ca<sup>++</sup> levels (<sup>#</sup>P<0.001 vs VEH, N=4-17).



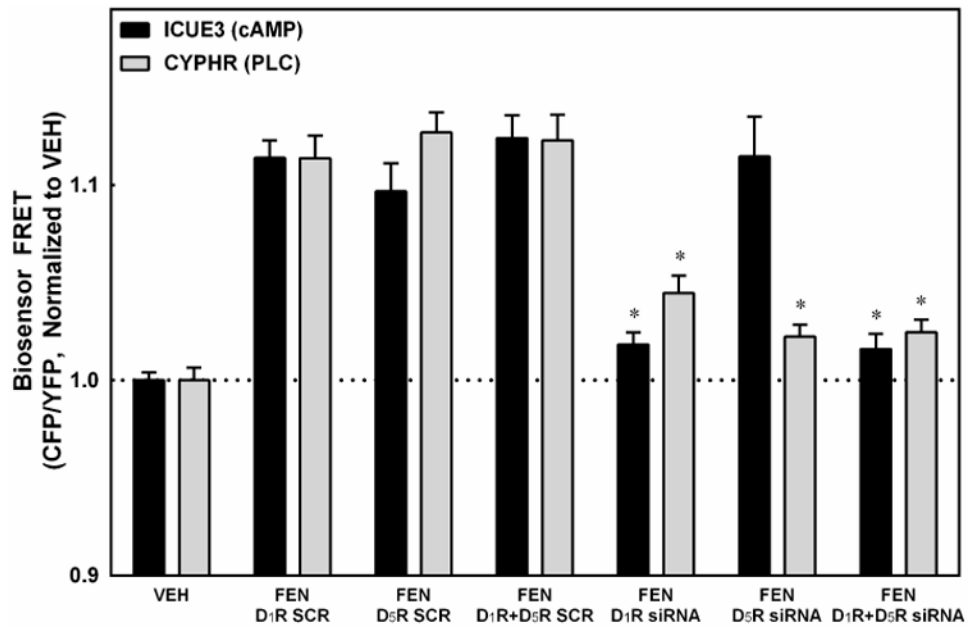


**Figure 5. D<sub>1</sub>R vs. D<sub>5</sub>R siRNA Effects on AC and PLC pathways**

D<sub>1</sub>R siRNA blocked the fenoldopam (FEN, D<sub>1</sub>R/D<sub>5</sub>R agonist) -stimulated increases in cAMP level and PLC activity (\*P<0.05 vs SCR, N=16 for ICUE3, N=4 for CYPHR). D<sub>5</sub>R siRNA blocked only the PLC effect (\*P<0.05 vs SCR, N=4), and the combination of the D<sub>1</sub>R and D<sub>5</sub>R siRNAs blocked both pathways (\*P<0.05 vs SCR, N=14 for ICUE3 and N=4 for CYPHR).

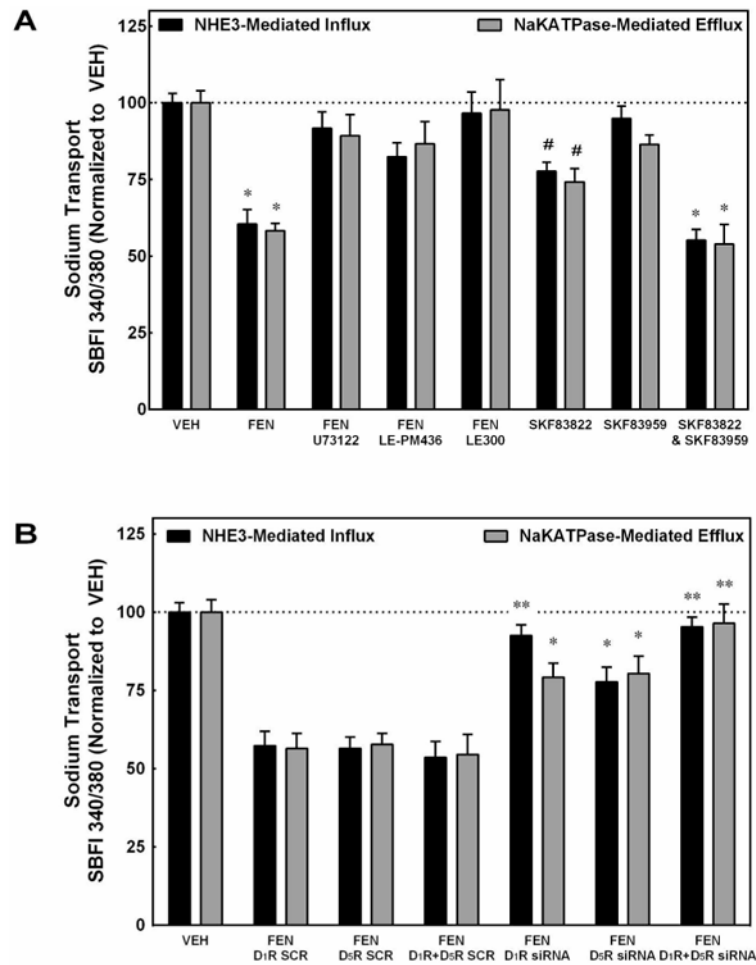


**Figure 6. Sodium Transport Assays**

**PANEL A:** The D<sub>1</sub>R/D<sub>5</sub>R agonist fenoldopam (FEN, 1  $\mu$ mol/L, 30 min) inhibited both NHE3-mediated sodium influx and NaKATPase-mediated sodium efflux in immortalized RPTCs (\* $P$ <0.0001 vs VEH, N=6). The co-addition of U73122 (PLC inhibitor, 10  $\mu$ mol/L), LE-PM436 (D<sub>5</sub>R-specific inhibitor, 1 nmol/L), or LE300 (D<sub>1</sub>R/D<sub>5</sub>R antagonist, 10  $\mu$ mol/L) returned the sodium influx and efflux to VEH levels. The AC-specific activator SKF83822 (10  $\mu$ mol/L, 20 min) inhibited both NHE3 and NaKATPase (# $P$ <0.001 vs VEH, N=6). The PLC-specific activator SKF83959 (10  $\mu$ mol/L, 20 min) did not inhibit either NHE3 or NaKATPase but the combination of SKF83822 and SKF83959 inhibited both NHE3 and NaKATPase and to a greater extent than SKF83822 alone (\* $P$ <0.0001 vs VEH, N=6).

**PANEL B:** The FEN-mediated inhibition of sodium efflux can be partially reversed by siRNA specific to D<sub>1</sub>R or D<sub>5</sub>R, or fully reversed by the combination of D<sub>1</sub>R and D<sub>5</sub>R siRNAs (\* $P$ <0.05 vs SCR, \*\* $P$ <0.001 vs SCR, N=6). D<sub>1</sub>R siRNA alone reversed sodium influx as effectively as the combination of the D<sub>1</sub>R and D<sub>5</sub>R siRNAs.

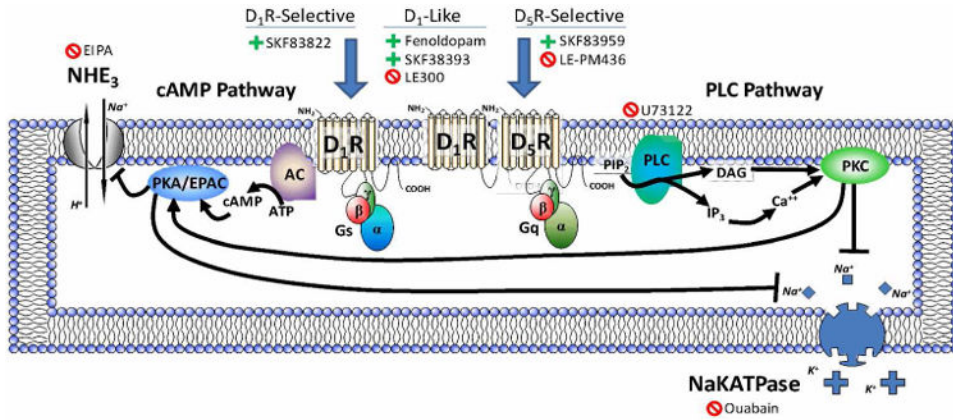


**Figure 7.** This model lists the D<sub>1</sub>R and D<sub>5</sub>R agonists and inhibitors and depicts our proposed pathways and heteromeric structure in relation to signaling and regulation of sodium transport in a human renal proximal tubule cell (RPTC). D<sub>1</sub>R signaling through adenylyl cyclase (AC) and cAMP and PKA or EPAC (exchange protein activated by cAMP) can inhibit both NHE3 and NaKATPase, while the heteromeric D<sub>1</sub>R/D<sub>5</sub>R complex signaling through PLC acts to positively modulate the D<sub>1</sub>R activity. In RPTCs, SKF83822, which stimulates adenylyl cyclase (AC), may be a D<sub>1</sub>R selective agonist while SKF83959, which stimulates phospholipase C (PLC), may be a D<sub>5</sub>R selective agonist and inhibited by LE-PM436, the newly described D<sub>5</sub>R-selective antagonist. Fenoldopam and SKF8393 stimulate both D<sub>1</sub>R and D<sub>5</sub>R while LE300 inhibits both D<sub>1</sub>R and D<sub>5</sub>R. U73122 inhibits PLC activity, ouabain inhibits NaKATPase activity and EIPA inhibits NHE3 activity.